# Origins of Regio- and Stereochemistry in Type 2 Intramolecular *N*-Acylnitroso Diels−Alder Reactions: A Computational Study of Tether Length and Substituent Effects

Leah Cleary, Victor W. Mak, Scott D. Rychnovsky,* Kenneth J. Shea,* and Nicholas Sizemore

Department of Chemistry, 1102 Natural Sciences II, University of California, Irvine, California 92697-2025, United States

Ⓢ Supporting Information

ABSTRACT: Quantum mechanical calculations have been used to investigate type 2 intramolecular *N*-acylnitroso Diels−Alder reactions. Experimentally observed regioselectivities and diastereoselectivities of these reactions have been reproduced using B3LYP/6-31+G(d) DFT calculations. The factors that govern selectivity (i.e., tether length, tether substitution and diene substitution) were systematically investigated. Tethers less than 6 carbon atoms lead to 1,3-regioisomers due to conformational restrictions. Substituents on the tether lead to diastereoselective outcomes dictated by transannular interactions in the transition states. The modest diastereoselectivity of diene-substituted substrates is rationalized as arising from reduction of eclipsing interactions in the flattened diene transition states. This method should prove valuable for planning syntheses involving type 2 intramolecular Diels−Alder reactions.

DFT calculations predict observed selectivities
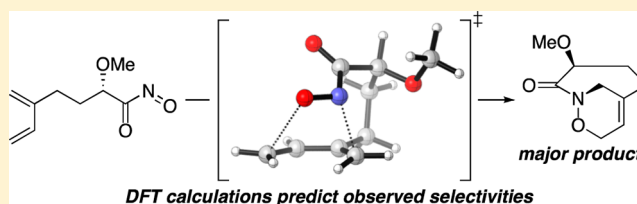
INTRODUCTION

The type 2 intramolecular Diels−Alder (T2IMDA) reaction involves the union of a diene and a dienophile that are tethered at the C2 position of the diene to afford bicyclic bridgehead alkene products (Figure 1).[1−3] This reaction can either afford
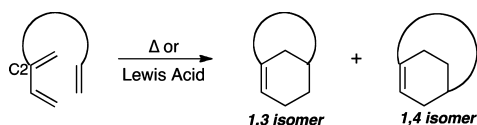

Figure 1. Regioselectivity of the T2IMDA.

1,3- or 1,4-regioisomers as products, which is largely dependent upon the length or rigidity of the tether. The regiochemical nomenclature is determined by counting along the newly formed ring from the bridgehead alkene to the other end of the tether.

The T2IMDA reaction is a powerful method for the construction of polycyclic frameworks that has found utility in the synthesis of challenging bridgehead olefins and complex organic molecules (Scheme 1). Schreiber and Kiessling's approach to esperamicin attempted to employ a T2IMDA reaction to access the cyclohexenyl core of the molecule. Though the rigid ene-diyne substrate was originally reported to afford the desired 1,3-regioisomer, subsequent synthetic studies and NMR experiments revealed that the major product was in fact the 1,4-regioisomer.[4,5] In contrast, the synthesis of taxadienone features a Lewis acid promoted T2IMDA reaction to afford the taxane core in a highly diastereoselective manner.[6] More recently, Stoltz and Hong utilized a related IMDA reaction to assemble the tricyclic core of 9β-presilphiperfolan-

Scheme 1. Application of the T2IMDA Reaction to Complex Products
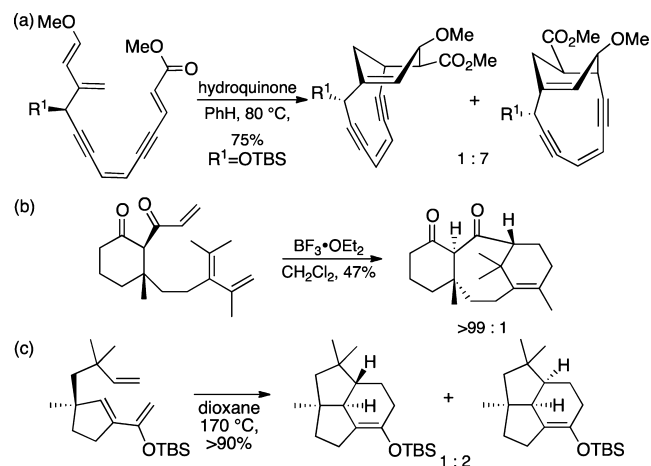
1α-ol, which proceeded in high yield but afforded the desired diastereomer as the minor product.[7]

These examples highlight two important facts. First, the T2IMDA reaction is a powerful method for the rapid synthesis of complex architectures. Second, the regio- and stereochemical outcomes of these reactions can be challenging to predict. With the second point in mind, we set out to develop a simple computational method for predicting product distributions in T2IMDA reactions.

In this report we provide an analysis of contributing factors to the regio- and stereoselectivity of the T2IMDA reaction. The *N*-acylnitroso T2IMDA reaction was chosen for this computational study since this reaction has provided a wealth of experimental data concerning both regio- and diastereoselectivities.[8−10] The computational method accurately describes the observed product distributions and identifies contributing factors to regio- and stereochemistry.

Hetero-Diels−Alder reactions of *N*-acylnitroso dienophiles have been useful tools for the synthesis of biologically active molecules.[11] The *N*-acylnitroso T2IMDA reaction has been studied as a method to synthesize medium ring lactams and *cis*-1,4-cyclohexyl aminoalcohols.[8] This reaction is attractive because it employs synthetically tractable precursors (diene esters) to assemble complex cycloadducts that can be further functionalized (Figure 2). The increased reactivity of the *N*-
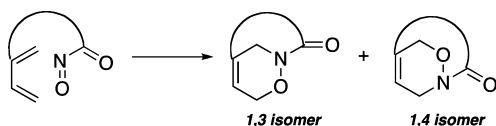

Figure 2. Regioselectivity of the *N*-acylnitroso T2IMDA.

acylnitroso moiety allows these reactions to proceed under ambient or even cryogenic temperatures without the use of Lewis acids, a feature absent from the all-carbon T2IMDA reactions.

We have employed density functional theory (DFT) calculations in an effort to understand the observed regio- and stereochemical outcomes of the *N*-acylnitroso T2IMDA reaction. In particular, we have sought to understand how subtle changes in tether length and substitution play a dramatic, nonobvious role in determining the stereochemical outcome of these reactions. Tether length was investigated to determine the regiochemical reliability of the method, whereas tether and diene substitution were investigated to determine stereochemical reliability. The method described herein correlates well with experimental data and provides insight into predicting outcomes of these important reactions.

■ BACKGROUND

Scope of the *N*-Acylnitroso T2IMDA Reaction. Several factors including tether length and substitution, as well as diene substitution, have been shown experimentally to affect product distributions in this reaction. Tether length plays an important role for the regiochemical product distribution of the *N*-acylnitroso T2IMDA reaction (Table 1).[8,9] The cycloaddition

Table 1. Acyclic Diene *N*-Acylnitroso T2IMDA Reactions[9]

entry	*n*	conditions	% yield	ratio (**2:3**)
1	1 (**1a**)	Et$_4$NIO$_4$, CHCl$_3$, 0 °C	75	>95:5
2	2 (**1b**)	Et$_4$NIO$_4$, CHCl$_3$, 0 °C	80	>95:5
3	3 (**1c**)	Et$_4$NIO$_4$, CHCl$_3$, 0 °C	not isolated	N/A
4	3^a (**1d**)	PhH, 80 °C	60	50:50

^{a}Starting material was the dimethylanthrecene adduct of the acylnitroso diene.

of dienes and nitroso groups with 4- or 5-carbon tethers (**1a**, **1b**) results in exclusive formation of the 1,3-regioisomers (**2**). The standard reaction conditions failed to provide products in the 6-carbon tethered case (entry 3); however, upon masking the diene as the 9,10-dimethylanthracene adduct (**1d**), thermolysis led to a 1:1 mixture of 1,3- and 1,4-regioisomers (entry 4). The regiochemical crossover with a tether of 6 or more carbons favors the electronically preferred 1,4-regioisomer (**3**) because of the increased flexibility of the tether. This change in regiomeric preference has also been observed in Lewis acid-catalyzed T2IMDA reactions.[12]

The stereochemistry of *N*-acylnitroso T2IMDA reactions is influenced by substitutions on the tether.[8] Of particular interest was the stereochemical reversal of product distribution in α-carbonyl substituted cases (Table 2). Alkyl α-substituents, such as benzyl or allyl groups, afforded diastereomer **5** exclusively with an *anti* relationship between the substituent and the bridging carbon (entries 1 and 2). In contrast, ethereal α-substituents, such as benzyl or *tert*-butyldiphenylsiloxy ethers, provide *syn* diastereomer **6** as the predominant product (entries 3 and 4). The preferential formation of the *syn* diastereomer in ethereal cases was originally hypothesized to be a manifestation of a dipole minimization in the transition state. However, ethereal substrates showed negligible changes in diastereoselectivity across solvents of varying polarity, indicating that the observed selectivity was not correlated to dipole minimization.
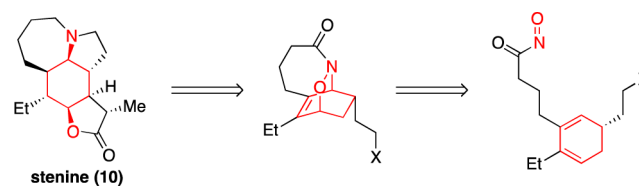
Table 2. α-Substituted Acyclic Diene *N*-Acylnitroso T2IMDA Reactions[8]

entry	R	% yield	*anti:syn* (**5:6**)
1	Bn (**4a**)	83	>95:5
2	allyl (**4b**)	70	>95:5
3	OBn (**4c**)	62	<5:95
4	OTBDPS (**4d**)	70	16:84

Table 3. Cyclic Diene *N*-Acylnitroso T2IMDA Reactions[10]

entry	R	% yield	*trans:cis* (**8:9**)
1	H (**7a**)	50	N/A
2	CH$_2$CH$_2$OTBS (**7b**)	50	86:14

Scheme 2. Retrosynthetic Analysis of Stenine
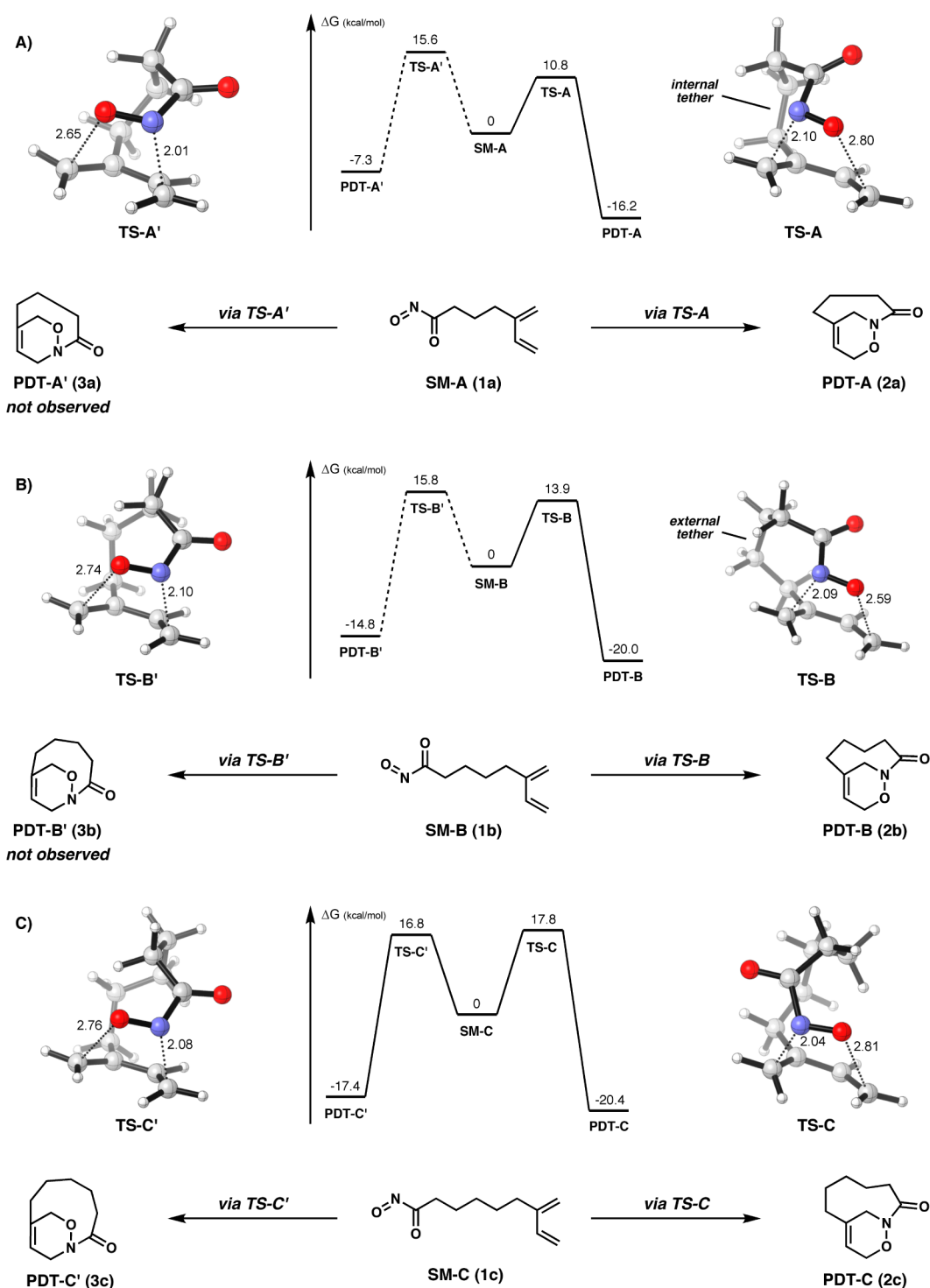

stenine (**10**)

Figure 3. Free energy diagrams and transition structures for acyclic dienes of carbon tether lengths 4−6 (A−C), calculated at the B3LYP/6-31+G(d) level. Forming bonds are shown as dotted lines, interatomic distances are given in Å, and free energies are given in kcal mol^{-1}. Experimentally unobserved pathways are shown as dashed lines. Nomenclature of tether orientation (internal vs external) is shown for illustrative purposes.

Cyclic diene substrates, both unsubstituted and substituted, have been previously investigated (Table 3). In both cases, the 1,3-regioisomer is obtained exclusively, and in the substituted example there is a preference for a *trans* relationship between the substituent and the newly formed bonds. These substituted dienes are model systems for the synthesis of several members of the stemona alkaloids, including stenine (Scheme 2).[10]

Previous Theoretical Studies. Comparisons of quantum mechanical methods for studying pericyclic reaction mechanisms, including intermolecular Diels−Alder reactions, have been reported.[13] A subsequent computational study by Leach and Houk describes the transition state and mechanism of intermolecular hetero-Diels−Alder reactions, including *N*-acylnitroso examples.[14] The study concluded that these reactions proceed through a concerted, yet highly asynchro-
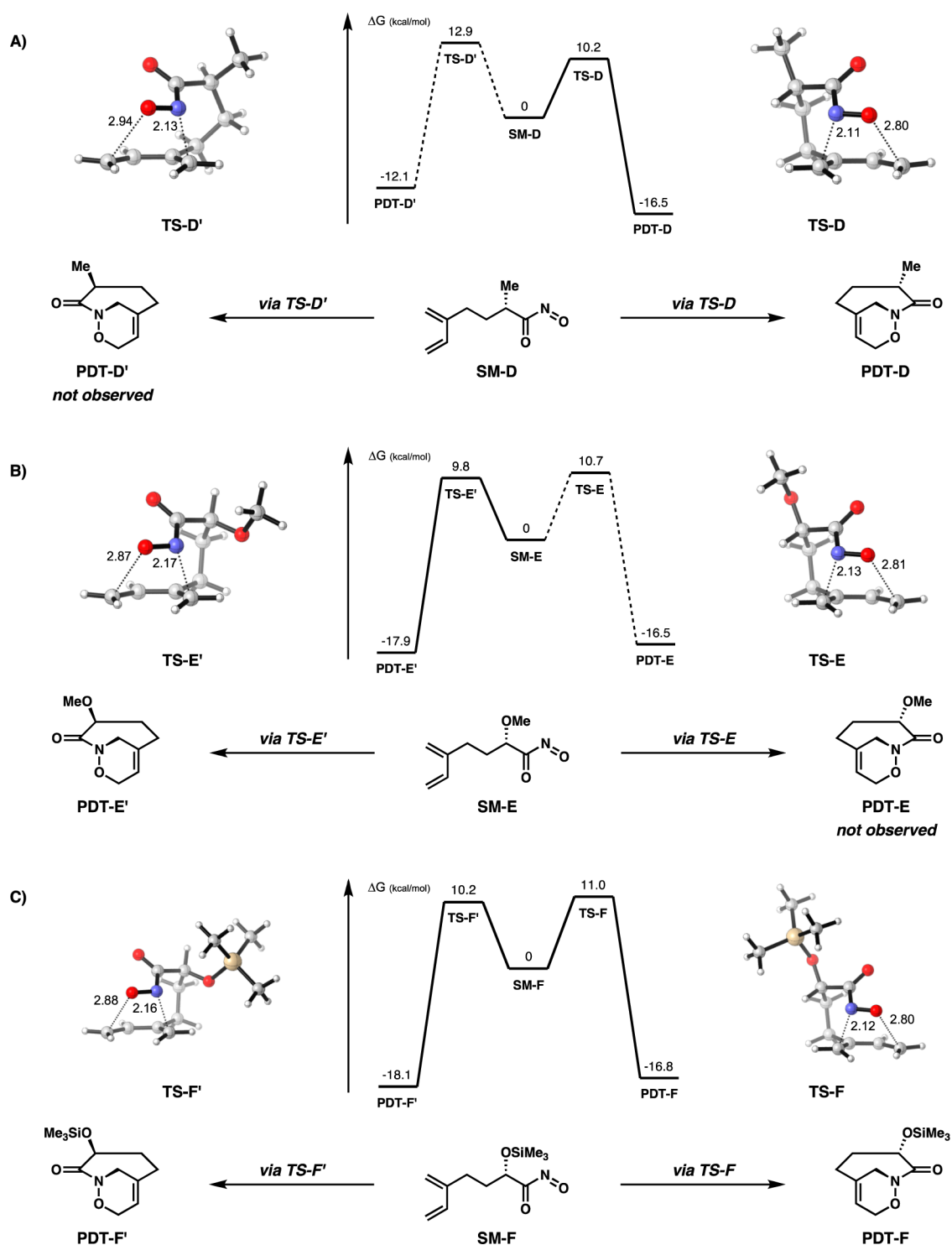
Figure 4. Free energy diagrams and transition structures for the stereoselectivity (*syn* vs *anti*) of acyclic diene substrates with α-methyl (A) or α-ethereal (B,C) substituted tethers, calculated at the B3LYP/6-31+G(d) level. Forming bonds are shown as dotted lines, interatomic distances are given in Å, and free energies are given in kcal mol⁻¹. Experimentally unobserved pathways are shown as dashed lines.

nous, *endo* transition state. While type 1 intermolecular Diels–Alder (T1IMDA) have been extensively studied computationally,[15−21] there have been no computational studies of either the T2IMDA reaction or *N*-acylnitroso T2IMDA reaction.

■ COMPUTATIONAL METHODS

Conformational analysis of starting materials and products were performed in Spartan '08[22] using MMFF.[23] Geometry optimization,

transition state identification, and vibrational frequency analysis were carried out with Gaussian 09[24] using B3LYP/6-31+G(d)[25,26] as convergent, gas-phase calculations performed at 273 K. Transition states were confirmed by IRC calculations.[27] Free energies are reported from the unscaled frequencies. Graphics were generated using the CYLview program.[28]
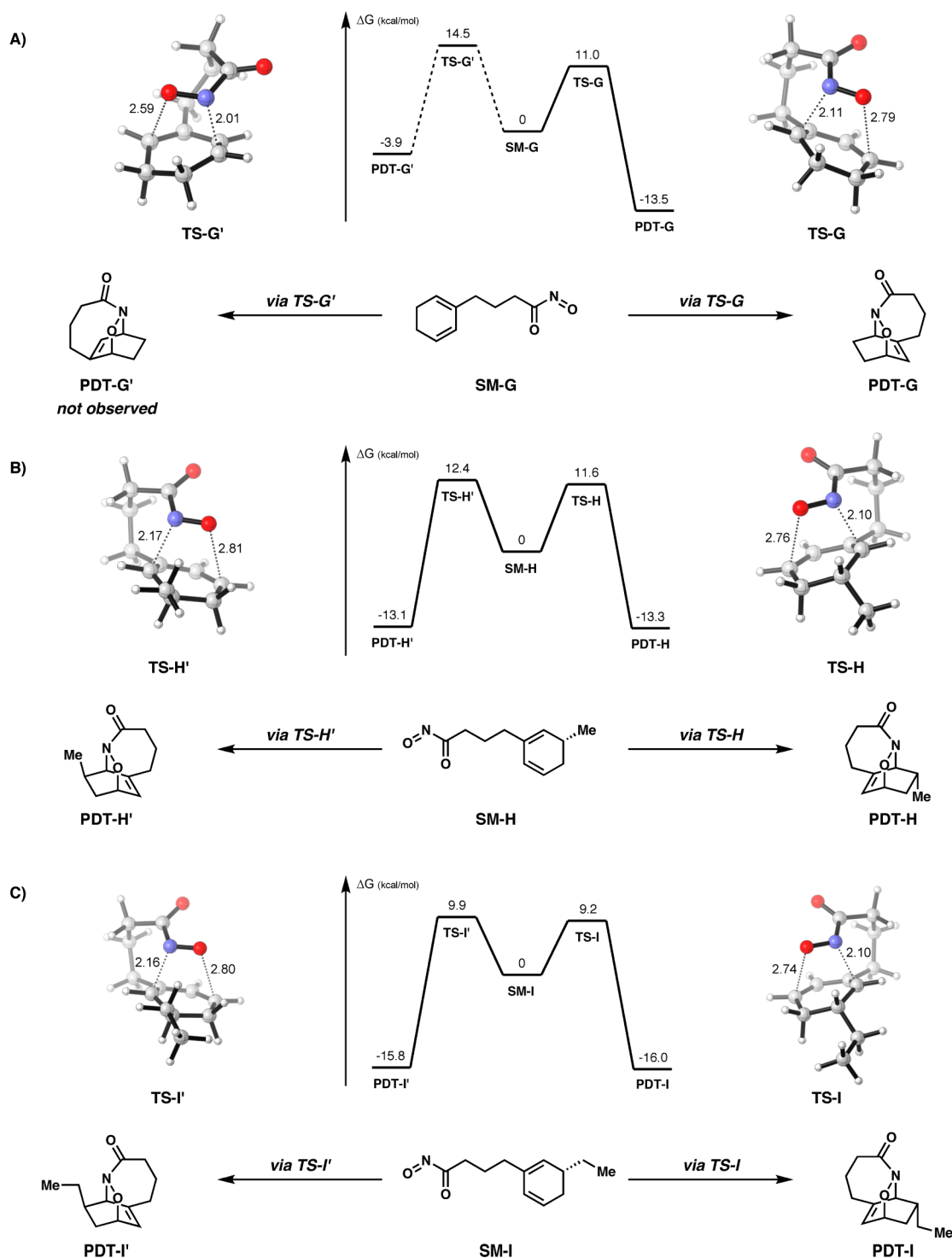
Figure 5. Free energy diagrams and transition structures for the regioselectivity (1,3 vs 1,4) of unsubstituted cyclic diene substrate (A) and stereoselectivity (*cis* vs *trans*) of substituted cyclic diene substrate (B,C), calculated at the B3LYP/6-31+G(d) level. Forming bonds are shown as dotted lines, interatomic distances are given in Å, and free energies are given in kcal mol^{-1}. Experimentally unobserved pathways are shown as dashed lines.

■ RESULTS

Acyclic Dienes and the Role of Tether Lengths in Product Distribution. The calculated energy diagrams and transition states for the acyclic diene *N*-acylnitroso T2IMDA reaction for 4-, 5- and 6-carbon tethered substrates are shown in Figure 3. The reaction is highly exothermic, with a late transition state, which resembles the products. In the case of 4-

carbon tether **SM-A**, the 1,3-regioisomeric **TS-A** is 4.8 kcal mol^{-1} lower in energy than the 1,4-regioisomeric **TS-A′**. A comparison of C−N distances in the transition states shows less advanced bond formation in the lower energy **TS-A** than in **TS-A′** (2.10 vs 2.01 Å). Both TSs display a high level of asychronicity, as evident by the large differences between the C−O and C−N bond distances (2.80 vs 2.10 Å for **TS-A**). The 7-membered ring resulting from C−N bond formation of **TS-A**

adopts a chair geometry, whereas the 8-membered ring of **TS-A′** is a chair−boat conformation. In both cases, these conformations result in the tether β-carbon oriented away from the C1 carbon of the adjacent diene terminus (internal orientation). The free energy of **PDT-A′** is also dramatically higher than **PDT-A** (8.9 kcal mol^{-1}).

Extending the tether length to 5-carbons results in a smaller $\Delta\Delta G^{\ddagger}$ (1.9 kcal mol^{-1}) between **TS-B** and **TS-B′**, favoring 1,3-regioisomeric **TS-B**, in contrast to $\Delta\Delta G^{\ddagger}$ of **TS-A** and **TS-A′** (4.8 kcal mol^{-1}). As compared to the chair structure adopted by **TS-A**, **TS-B** tether must adopt a chair−boat conformation where the tether β-carbon is oriented toward the C1 carbon of the adjacent diene terminus (external tether). As a result of this orientation, A^{1,3} strain between the γ-carbon of the tether and C1 of the diene destabilizes **TS-B** compared to **TS-A**. Formation of the C−O bond is more advanced in **TS-B** than **TS-B′** (2.59 vs 2.74 Å), and the difference in free energies of **PDT-B** and **PDT-B′** (5.2 kcal mol^{-1}) is less than in the 4-carbon tether example.

When the tether length is extended to 6-carbons, the 1,4-regioisomeric **TS-C′** is now 1.0 kcal mol^{-1} lower in energy than the 1,3-regioisomeric **TS-C**. Higher activation energies are required for these pathways compared to the 4- and 5-carbon tether cases (by 2.9−7.0 kcal mol^{-1}). Distances between each pair of atoms undergoing new bond formation are similar in both **TS-C′** and **TS-C**, which also both exhibit asynchronous bond formation. **TS-C′** adopts an internal tether orientation, while **TS-C** possesses an external tether orientation; however, there are limited steric interactions in **TS-C** as compared to **TS-B** because of the flexibility of the long tether.

Diastereoselectivity of α-Substituted Tether Substrates. The calculated energy diagrams and transition states for the *N*-acylnitroso T2IMDA reaction with α-substituted substrates are shown in Figure 4. In the case of substrate **SM-D** (analogous to Table 2, entries 1 and 2) with a methyl group α to the acylnitroso, **TS-D** leading to the *anti*-diastereomer is 2.7 kcal mol^{-1} lower in energy than the *syn*-diastereomeric **TS-D′**. Both TSs display a high level of asychronicity; however, **TS-D** exhibits an internal tether orientation, whereas the tether in **TS-D′** is arranged in an external orientation. This conformation places the γ-hydrogen of **TS-D′** in direct proximity of the terminal olefin, causing a net destabilizing effect. Because the internal tether is favored, the *anti*-diastereomer is predicted, which reflects the experimental results that benzyl substituted **5a** or allyl substituted **5b** are obtained as single diastereomers.

The models with ethereal α-substituents (**SM-E** and **SM-F**) are similar to each other and are in direct contrast to α-methyl substrate **SM-D**. Both **TS-E′** and **TS-E** adopt internal tether orientations as well as display similar levels of asychronicity and bond development. For ethereal substrates **SM-E** and **SM-E′** (analogous to Table 2, entry 3), $\Delta\Delta G^{\ddagger}$ has decreased to 0.9 kcal mol^{-1}, and *syn*-diastereomeric pathway through **TS-E′** is now preferred. Similarly, **TS-F′** and **TS-F** (analogous to Table 2, entry 4) adopt internal tether orientations with a $\Delta\Delta G^{\ddagger}$ of 0.8 kcal mol^{-1}, and again the *syn*-diastereomeric pathway through **TS-F′** is preferred. All transition states for the ethereal substrates possess a tether in an internal orientation, and there is only a slight energetic preference for the *syn*-diastereomers. Nevertheless, the model accurately predicts the major products from the cycloadditions leading to substrates such as benzyl ether **4c** or *tert*-butyldiphenylsiloxy ether **4d**.

Cyclic Dienes and Product Distributions. Calculated energy diagrams and transition states for the cyclic diene *N*-

acylnitroso T2IMDA reactions are shown in Figure 5. Similar to the acyclic diene with a 4-carbon tether (**TS-A**), **TS-G** is 3.5 kcal mol^{-1} lower in energy than the **TS-G′**, favoring the 1,3-regioisomer. Both TSs display a high level of asychronicity, internal tether orientation, and as in the acyclic 4-carbon case, the free energy of **PDT-G′** is dramatically higher than **PDT-G** (ΔG = 9.6 kcal mol^{-1}).

Substituted cyclic diene substrates **SM-H** and **SM-I** were examined for diastereoselectivity. Both data sets have very similar characteristics; the $\Delta\Delta G^{\ddagger}$ between *cis* and *trans* TSs is small (Me = 0.8 kcal mol^{-1}, Et = 0.7 kcal mol^{-1}), favoring the *trans* product. Formation of the C−N bond is slightly more advanced in **TS-H** than **TS-H′** (2.10 vs 2.17 Å), though the interatom distances of the developing bonds in the Me and Et cases are similar to **TS-G**. The small magnitude of $\Delta\Delta G^{\ddagger}$ for **TS-I** and **TS-I′** accurately predicts the 6:1 ratio of diastereomers and thus the stereochemical outcome of the cycloaddition of **7b**.

■ DISCUSSION

Tether Length Dictates Regiochemistry. The regiochemical outcome (1,3 vs 1,4 product formation) is largely dictated by the nature of the tether, where the increased flexibility afforded by a longer tether lowers the energy of the TS leading to the 1,4 product. For even numbered tethers (i.e., 4- and 6-carbon cases), TSs leading to 1,3 products proceed through an internal tether orientation in order to reduce eclipsing interactions. In contrast, TSs leading to 1,3 products for odd numbered tethers (5-carbon case) adopt an external conformation. While this conformation reduces eclipsing interactions in the tether, it also raises the energy of the TS by introducing an A^{1,3} interaction between the tether and the diene. The calculations comparing cycloaddut precursors with tether lengths of 4 and 5 carbons to a substrate with 6 carbons unequivocally confirm that the strain imparted by the tether causes the reaction to prefer the 1,3-regioisomeric product in the 4 and 5 carbon cases.

Cycloadduct Olefin Strain: Comparison of Calculated and X-ray Geometries. To confirm the accuracy of this computational method, the calculated geometry of the products in the unsubstituted acyclic cases were compared to the X-ray crystallographic data. In particular, the torsional angles (τ) and pyrimidalization angles (χ) about the bridgehead olefin and the bridgehead amide were calculated as previously described by Winkler and Dunitz (Figure 6).[29] An unstrained sp^2 alkene, such as ethene, is expected to have each substituent 90° to the π system and thus τ, χ_{C1}, and χ_{C2} all equal to zero. So-called "twist amides"[30] represent extremely strained systems, such as 1-aza-2-adamantanone[31,32] or 2-quinuclidone,[33] where the π orbitals are virtually perpendicular to each other ($\tau \approx 90°$). An accurate computational method would describe the molecules
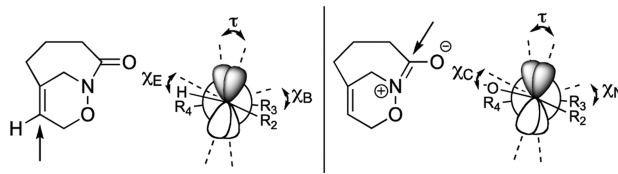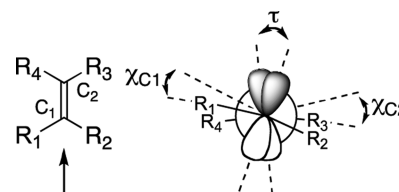

Figure 6. A visual description of Dunitz's model of olefin strain, where τ describes the torsional strain between the π orbitals and χ_C is a measure of the pyrimidalization of the sp^2 center.

so that the difference in the angles between the computational and X-ray data (Δ) would be zero.

The computed angles describing the olefin and amide for each of the 1,3 cycloadducts, as well as the deviation from experimental angles are shown in Table 4. In all cases, the difference between the computational and experimental angles is small (Δ ≤ 4.4°), supporting the validity of the computational method. These data also show that as tether length is increased, the olefin adopts a more sp^2-like geometry as indicated by the decrease in the torsional angle of the olefin. The computational angles for the 6-carbon tethered 1,4-regioisomeric product (**3c**) show a much greater torsional strain about both the olefin and the amide than the 1,3 products (**2a−c**). These angles represent the physical limit of allowed strain in these systems as synthesized by the T2IMDA because the 1,4 products for the 4- and 5-carbon tethers are not observed experimentally.

Table 4. Computational Angles and Deviation from Experimental Angles (Δ) of Acyclic Diene Cycloadducts

		comp.	Δ		comp.	Δ
2a	χ_B	23.4°	3.1°	χ_N	54.5°	−0.3°
	χ_E	11.3°	2.3°	χ_C	0.4°	0.0°
	τ_{olefin}	6.95°	0.1°	τ_{amide}	3.20°	−0.3°
2b	χ_B	14.1°	0.6°	χ_N	53.2°	0.6°
	χ_E	8.4°	4.4°	χ_C	1.1°	−0.4°
	τ_{olefin}	3.7°	0.1°	τ_{amide}	10.70°	0.4°
2c	χ_B	9.3°	−1.9°	χ_N	47.5°	−1.5°
	χ_E	4.8°	−1.6°	χ_C	2.8°	−1.3°
	τ_{olefin}	2.25°	−0.9°	τ_{amide}	15.35°	−1.1°
3c	τ_{olefin}	11.3°	N/A	τ_{amide}	19.7°	N/A

Transannular Interactions Drive *syn*/*anti* Diastereoselectivity. Our model indicates the diastereoselectivity of tether-substituted substrates is controlled through steric interactions in the transition state. Substrates with alkyl substitution α to the acyl-nitroso group preferentially form the *anti* cycloadducts, whereas ether substitution favors *syn* products. The rest of the tether is not an innocent bystander and must be in the internal conformation to avoid steric interactions with the diene. Further tether substitution and substituents such as alkenes and alkynes will likely cause an impact on the diastereoselectivity and will be the topic of future studies.

A comparison of α-substituted TSs leading to *syn* products is shown in Figure 7. The α-Me substrate prefers to adopt an external orientation of the tether (**TS-D′**) in order to avoid a steric interaction (2.12 Å) between the terminal diene hydrogen and the methyl hydrogen present in the internal tether orientation (**TS-D″**). This close contact interaction is analogous to a *syn* pentane interaction and is more energetically disfavored than the allylic-type close contact interaction (2.08 Å) present in **TS-D′**, which is 1.0 kcal mol⁻¹ lower in energy than **TS-D″**. Interestingly, the external orientation TS also was identified in the unsubstituted 4-carbon tether and was 2.2 kcal mol⁻¹ higher in energy than the internally oriented **TS-A**. In
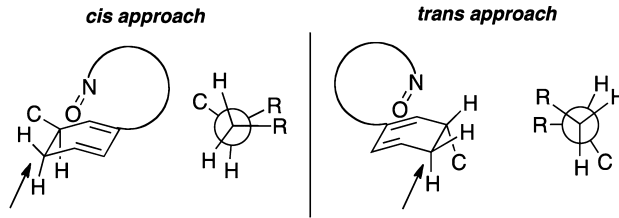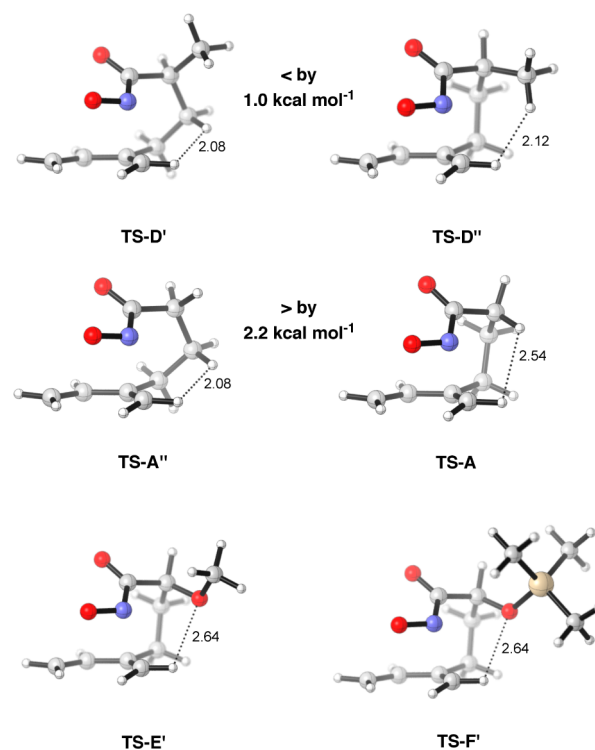

Figure 7. Comparison of external (left) and internal (right) transition structures for α-methyl substituted tether (**TS-Ds**), the analogous unsubstituted transition structures (**TS-As**), and the internal α-ethereal substituted tethers (**TS-E** and **TS-F**). Interatomic distances relevant to close contact interactions are given in Å and depicted as dotted lines.

contrast, the ether **TS-E′** and silyl ether **TS-F′** are able to accommodate an internal orientation because of the reduced steric demand of ether substitution as opposed to alkyl substituted **TS-D″**.

Diene Substitution Has Modest Effects on *cis*/*trans* Diastereoselectivity. While there is a clear preference for the formation of 1,3-regioisomeric products in the case of cyclic dienes (Figure 5a), substituted dienes show only a modest preference for *trans* products (Figure 5b and c). The less than expected magnitude of ΔΔG‡ as well as the calculated and experimental diastereoselectivities resulting from diene substitution may be rationalized by examining various physical parameters influencing the transition states. The concerted, highly asynchronous, nature of the transition states result in C−N bond formation preceding C−O bond formation. Conformational restrictions of the cyclic diene also limit the torsional freedom of substituents on the diene. As a result, *trans* approach TSs (Table 5, entries 1 and 3), while sterically less demanding, are required to adopt a more eclipsed conformation than *cis* approach TSs (entries 2 and 4). This eclipsed conformation flattens the diene and effectively raises the free energy of the *trans* approach pathway.

Experimental studies have shown that the regio- and stereochemical outcomes of *N*-acylnitroso T2IMDA reactions are attributable to tether length and substituent effect, respectively. This study has identified a computational method that accurately describes the observed product distributions (Table 6). Tether length studies show the appropriate regiochemical crossover (at tether length = 6-carbon), and the computational products are in good agreement with the X-ray crystallographic data. Studies of substrates with α-

Table 5. Comparison of Dihedral Angles from *cis* and *trans* Approaches in Substituted Cyclic Diene Substrates

entry	structure/approach	dihedrals			
		R–R	C–H	H–H	average
1	TS-H/*trans*	2.6°	5.5°	8.0°	5.4°
2	TS-H′/*cis*	14.1°	21.9°	23.1°	19.7°
3	TS-I/*trans*	6.0°	10.1°	12.2°	9.4°
4	TS-I′/*cis*	13.5°	21.5°	22.5°	19.2°

Table 6. Summary of Computed Substrate Selectivities in Terms of $\Delta\Delta G^{\ddagger}$ (in kcal/mol) and Product Distributions (Experimental Values in Parentheses)

entry	substrate	selectivity	$\Delta\Delta G^{\ddagger}$ DFT (expt)	distr DFT (expt)
1	**1a**	1,3:1,4	4.8 (>1.6)	>99:1 (>95:5)
2	**1b**	1,3:1,4	1.9 (>1.6)	>97:3 (>95:5)
3	**1c**	1,3:1,4	−1.0 (0)	20:80 (50:50)
4	**7a**	1,3:1,4	3.5 (>1.6)	>99:1 (>95:5)
5	**4a**	anti:syn	2.7 (>1.6)	>99:1 (>95:5)
6	**4b**	anti:syn	2.7 (>1.6)	>99:1 (>95:5)
7	**4c**	anti:syn	−0.9 (< −1.6)	19:81 (<5:95)
8	**4d**	anti:syn	−0.8 (−0.9)	22:78 (16:84)
9	**7b** (SM-H)	trans:cis	0.8 (0.97)	78:22 (86:14)
10	**7b** (SM-I)	trans:cis	0.9 (0.97)	73:25 (86:14)

substitution also agree with the experimental results that carbon-linked substituents lead to *anti*-products, while oxygen-linked substituents afford *syn*-products. Perhaps more importantly, these studies revealed that tether-diene steric interactions, not dipole minimization, give rise to the observed stereoselectivity. Studies of cyclic diene systems have also recapitulated experimental results with regard to regio- and stereoselectivity. These studies suggest the modest stereoselectivity is a result of the required eclipses conformation that the less hindered *trans* product must adopt in the transition state.

CONCLUSION

These computational studies have demonstrated that the T2IMDA reaction can be effectively modeled using density functional theory. As a result, current efforts to model other classes of T2IMDA reactions and additional tether substitution patterns are underway. We believe this computational study will provide a simple method to predict complex *N*-acylnitroso, and other T2IMDA reactions, which will lead to a broader applicability of these synthetically useful reactions.

ASSOCIATED CONTENT

Ⓢ Supporting Information

Calculated geometries and energies, as well as complete references for Gaussian 09 and Spartan '08. This material is available free of charge via the Internet at http://pubs.acs.org.

AUTHOR INFORMATION

Corresponding Author
*E-mail: srychnov@uci.edu; kjshea@uci.edu.

Notes
The authors declare no competing financial interest.

ACKNOWLEDGMENTS

REFERENCES

(1) Bear, B. R.; Sparks, S. M.; Shea, K. J. *Angew. Chem., Int. Ed.* **2001**, *40*, 820−849.
(2) Shea, K. J.; Wise, S. *J. Am. Chem. Soc.* **1978**, *100*, 6519−6521.
(3) Shea, K. J.; Wise, S. *Tetrahedron Lett.* **1979**, *20*, 1011−1014.
(4) Schreiber, S. L.; Kiessling, L. L. *J. Am. Chem. Soc.* **1988**, *110*, 631−633.
(5) Schreiber, S. L.; Kiessling, L. L. *Tetrahedron Lett.* **1989**, *30*, 433−436.
(6) (a) Mendoza, A.; Ishihara, Y.; Baran, P. S. *Nat. Chem.* **2012**, *4*, 21−25. (b) Jackson, R. W.; Shea, K. J. *Tetrahedron* **1994**, *35*, 1317. (c) Winkler, J. D.; Kim, H. S.; Kim, S.; Ando, K.; Houk, K. N. *J. Org. Chem.* **1997**, *62*, 2957.
(7) Hong, A. Y.; Stoltz, B. M. *Angew. Chem., Int. Ed.* **2012**, *51*, 9674−9678.
(8) Sparks, S. M.; Chow, C. P.; Zhu, L.; Shea, K. J. *J. Org. Chem.* **2004**, *69*, 3025−3035.
(9) Sparks, S. M.; Vargas, J. D.; Shea, K. J. *Org. Lett.* **2000**, *2*, 1473−1475.
(10) Zhu, L.; Lauchli, R.; Loo, M.; Shea, K. J. *Org. Lett.* **2007**, *9*, 2269−2271.
(11) Bodnar, B. S.; Miller, M. J. *Angew. Chem., Int. Ed.* **2011**, *50*, 5630−5647.
(12) Shea, K. J.; Gilman, J. W. *Tetrahedron Lett.* **1983**, *24*, 657−670.
(13) Wiest, O.; Montiel, D. C.; Houk, K. N. *J. Phys. Chem. A* **1997**, *101*, 8378−8388.
(14) Leach, A. G.; Houk, K. N. *J. Org. Chem.* **2001**, *66*, 5192−5200.
(15) Tantillo, D. J.; Houk, K. N.; Jung, M. E. *J. Org. Chem.* **2001**, *66*, 1938−1940.
(16) Iafe, R. G.; Houk, K. N. *J. Org. Chem.* **2008**, *73*, 2679−2686.
(17) Paddon-Row, M. N.; Longshaw, A. I.; Willis, A. C.; Sherburn, M. S. *Chem.—Asian J.* **2009**, *4*, 126−134.
(18) Lilly, M. J.; Miller, N. A.; Edwards, A. J.; Willis, A. C.; Turner, P.; Paddon-Row, M. N.; Sherburn, M. S. *Chem.—Eur. J.* **2005**, *11*, 2525−2536.
(19) Paddon-Row, M. N.; Moran, D.; Jones, G. A.; Sherburn, M. S. *J. Org. Chem.* **2005**, *70*, 10841−10853.
(20) Cayzer, T. N.; Paddon-Row, M. N.; Moran, D.; Payne, A. D.; Sherburn, M. S.; Turner, P. *J. Org. Chem.* **2005**, *70*, 5561−5570.
(21) Pearson, E. L.; Willis, A. C.; Sherburn, M. S.; Paddon-Row, M. N. *Org. Biomol. Chem.* **2008**, *6*, 513−522.
(22) *Spartan'08*; Wavefunction, Inc.: Irvine, CA, 2008.
(23) Halgren, T. A. *J. Comput. Chem.* **1996**, *17*, 490−519.
(24) Frisch, M. J.; Trucks, G. W.; Schlegel, H. B.; Scuseria, G. E.; Robb, M. A.; Cheeseman, J. R.; Scalmani, G.; Barone, V.; Mennucci, B.; Petersson, G. A.; Nakatsuji, H.; Caricato, M.; Li, X.; Hratchian, H. P.; Izmaylov, A. F.; Bloino, J.; Zheng, G.; Sonnenberg, J. L.; Hada, M.; Ehara, M.; Toyota, K.; Fukuda, R.; Hasegawa, J.; Ishida, M.; Nakajima, T.; Honda, Y.; Kitao, O.; Nakai, H.; Vreven, T.; Montgomery, J. A., Jr.; Peralta, J. E.; Ogliaro, F.; Bearpark, M.; Heyd, J. J.; Brothers, E.; Kudin,

K. N.; Staroverov, V. N.; Kobayashi, R.; Normand, J.; Raghavachari, K.; Rendell, A.; Burant, J. C.; Iyengar, S. S.; Tomasi, J.; Cossi, M.; Rega, N.; Millam, J. M.; Klene, M.; Knox, J. E.; Cross, J. B.; Bakken, V.; Adamo, C.; Jaramillo, J.; Gomperts, R.; Stratmann, R. E.; Yazyev, O.; Austin, A. J.; Cammi, R.; Pomelli, C.; Ochterski, J. W.; Martin, R. L.; Morokuma, K.; Zakrzewski, V. G.; Voth, G. A.; Salvador, P.; Dannenberg, J. J.; Dapprich, S.; Daniels, A. D.; Farkas, Ö.; Foresman, J. B.; Ortiz, J. V.; Cioslowski, J.; Fox, D. J. *Gaussian 09*, Revision C.01; Gaussian, Inc.: Wallingford, CT, 2009.

(25) Becke, A. D. *J. Chem. Phys.* **1993**, *98*, 5648.

(26) Lee, C.; Yang, W.; Parr, R. G. *Phys. Rev. B: Condens. Matter Mater. Phys.* **1988**, *37*, 785−789.

(27) Gonzalez, C.; Schlegel, H. B. *J. Chem. Phys.* **1989**, *90*, 2154−2161.

(28) Legault, C. Y. *CYLview*, 1.0b; Université de Sherbrooke: Quebec, Canada, 2009; http://www.cylview.org.

(29) Winkler, F. K.; Dunitz, J. D. *J. Mol. Biol.* **1971**, *59*, 169−182.

(30) Aubé, J. *Angew. Chem., Int. Ed.* **2012**, *51*, 3063−3065.

(31) Kirby, A. J.; Komarov, I. V.; Wothers, P. D.; Feeder, N. *Angew. Chem., Int. Ed.* **1998**, *37*, 785−786.

(32) Kirby, A. J.; Komarov, I. V.; Feeder, N. *J. Chem. Soc., Perkin Trans. 2* **2001**, 522−529.

(33) Tani, K.; Stoltz, B. M. *Nature* **2006**, *441*, 731−734.